nature synthesis

Perspective

https://doi.org/10.1038/s44160-024-00600-x

Controlling the composition and elemental distribution of bi- and multi-metallic nanocrystals via dropwise addition

Received: 14 February 2024

Published online: 18 July 2024

Accepted: 6 June 2024

Check for updates

Chenxiao Wang ®¹, Jianlong He ®¹ & Younan Xia ®¹.² ⊠

Colloidal synthesis of metal nanocrystals often relies on using reduction kinetics to manipulate their size, shape, internal structure and composition. Whereas the first three features can all be readily manipulated, it remains challenging to control the composition of nanocrystals because the reduction rate, and thus the production rate of atoms, follows an exponential decay during the synthesis. By stabilizing the reduction rate of a precursor in the steady state, dropwise addition has emerged as a transformative route for the colloidal synthesis of nanocrystals. This Perspective highlights the advantages of dropwise addition over traditional one-shot injection for controlling the composition and elemental distribution of bi- and multi-metallic nanocrystals. Our analysis demonstrates the promise of dropwise addition for achieving the deterministic synthesis of complex nanocrystals with controlled compositions for a range of applications, especially those related to catalysis and energy conversion.

In the endeavour to tailor the properties of colloidal nanocrystals for specific applications, methods have been developed or refined for manipulating the size, shape, internal structure and composition of the nanocrystals¹. Despite major progress in recent years, the disparity between our capabilities in these domains of synthetic control remains, and disparity between domains has increased as control over certain synthetic domains (such as size) has become easier. Controlling the size of colloidal nanocrystals is relatively straightforward. The average size of nanocrystals has an inverse relationship with the number of seeds and is directly proportional to the amount of precursor added. To this end, decoupling growth from nucleation and successive seed-mediated growth have emerged as two simple and effective methods for precisely tuning the size of nanocrystals^{2,3}. It has been challenging to control the shape of nanocrystals, but over the past two decades, progressive understanding of the interplay between thermodynamic and kinetic parameters has enabled the development of many protocols to achieve intricate and diverse shapes for a multitude of nanocrystals, especially those made from noble metals⁴. A similar trend has also been established for controlling the internal structure⁵.

Among the four synthetic domains, composition may play the most critical role in determining the catalytic properties of nanocrystals. However, manipulating the composition experimentally, including the atomic ratio between different elements and their spatial distributions, remains a more abstruse scientific puzzle that is yet to be unravelled. The composition of nanocrystals did not attract substantial interest until the discovery of new optical and catalytic properties in systems that involve two different elements. For example, localized surface plasmon resonance is enhanced through incorporating Ag into the lattice of Au nanocrystals⁶, and highly active catalysts for oxygen reduction were discovered by alloying Pt with Ni or Co (ref. 7). These advances have triggered the exploration of composition, particularly surface composition, as an effective handle for tailoring the properties of metal nanocrystals. The recent trend towards the fabrication of catalysts based on 'high-entropy alloys' has further elevated the importance of composition control⁸.

¹School of Chemistry and Biochemistry, Georgia Institute of Technology, Atlanta, GA, USA. ²The Wallace H. Coulter Department of Biomedical Engineering, Georgia Institute of Technology and Emory University, Atlanta, GA, USA. —e-mail: younan.xia@bme.gatech.edu

As a prerequisite for composition control, it is crucial to understand how the composition of a nanocrystal evolves during synthesis. Understanding the intricate three-dimensional distribution of several elements within a nanocrystal presents a major technical challenge. Unlike size, shape or internal structure, visualizing or resolving the elemental distribution at an atomic scale is not straightforward. Although the overall composition of a batch of nanocrystals can be easily determined using techniques such as inductively coupled plasma mass spectrometry, the spatial distribution of each element at different sites of the same particle or among different particles can vary dramatically. The inhomogeneous distribution of elements among nanocrystals, coupled with the vital role of the surface in determining various crucial properties, highlights the need for an extensive analysis of the surface composition. Unfortunately, it remains challenging even with state-of-the-art characterization techniques. Although advanced microscopy tools have reached unprecedented spatial resolutions⁹, they still cannot reveal surface-specific information. On the other hand, surface-sensitive spectroscopy techniques yield only statistically averaged data¹⁰. Furthermore, the technical limitations and time-consuming nature of an instrumental analysis tend to make these methods more practical as supplementary tools for verifying scientific conclusions. To gain a thorough understanding of the composition and establish a general guideline for experimental control, we will examine the chemical reaction that governs the formation of nanocrystals, an often overlooked approach.

The most common route for preparing bi- and multi-metallic nanocrystals involves mixing the precursors with other reagents in a single solution to generate atomic building blocks through chemical reduction, where these building blocks subsequently undergo nucleation and growth to form nanocrystals¹¹. The resulting composition of the product is naturally determined by the relative rates at which these elemental species are produced and added onto the surface of a growing nanocrystal. Despite the potentially intricate mechanisms of nucleation and growth, the chemical reduction that is involved often exhibits a simple character. Considering noble metal nanocrystals as an example, the formation of each metal can be described as a second-order redox reaction between two reactants: the reductant and the precursor (or oxidant). The rate at which metal atoms are produced is governed by the rate law and is influenced by the concentrations of the two reactants. Consequently, it is conceivable to devise a strategy for achieving precise control over the precursor concentration, thereby ensuring that the reduction rate and the deposition rate of the corresponding metal atoms follow a predetermined ratio. By effectively manipulating the precursor concentration, we can ultimately achieve theory-based design and deterministic control over the composition of a nanocrystal. This approach highlights the potential to control the nanocrystal composition in a rational manner by implementing experimental control over the precursor concentration.

This Perspective focuses on an approach known as dropwise addition, which has the potential to revolutionize the synthesis of metal nanocrystals by controlling the reduction rates of different precursors in the steady state. A comprehensive comparison between the main features of one-shot injection and dropwise addition is presented to demonstrate the advantages offered by the latter. By conducting an in-depth analysis of the dropwise addition approach and its primary determinants, we identify two experimental parameters that enable tuning of the precursor concentration and therefore the on-demand design of nanocrystals. Using alloy nanocrystals as examples, we illustrate how these insights into the characteristics of chemical reactions, particularly the patterns of concentration variation, can accelerate the pursuit of the predictive synthesis of complex nanocrystals with desired compositions.

One-shot injection versus dropwise addition

In the conventional synthesis of metal nanocrystals, the precursor solution is usually injected into the reaction mixture in one shot

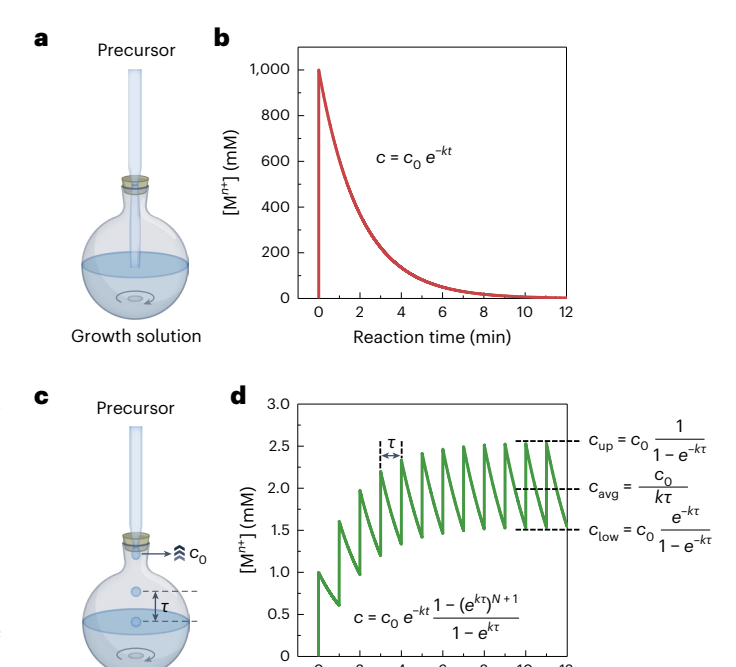


Fig. 1 | Comparison of one-shot injection with dropwise addition.

Growth solution

a, **b**, Experimental set-up for synthesis involving one-shot injection (**a**) and plot of the instantaneous concentration of the precursor as a function of the reaction time ($c_0 = 1 \, \text{M}, k = 0.5 \, \text{min}^{-1}$) (**b**). **c**, **d**, Experimental set-up for synthesis involving dropwise addition (**c**) and plot of the instantaneous concentration of the precursor as a function of the reaction time ($c_0 = 1 \, \text{mM}, k = 0.5 \, \text{min}^{-1}, \tau = 1 \, \text{min}$) (**d**). Note that the instantaneous concentrations (vertical axes) in **b** and **d** differ by several orders of magnitude between the two synthesis models, and c and c_0 are equivalent to [M^{n+1}] and [M^{n+1}]₀, respectively, where c_0 corresponds to the increase in concentration when all of the precursor solution is added in one shot (**a**,**b**) or when one droplet is added under dropwise addition (**c**,**d**).

Reaction time (min)

(Fig. 1a), followed by thermally triggered decomposition or reduction reaction(s) to trigger burst nucleation and then growth of the nanocrystals. As the energy barrier for nucleation is much greater than that for growth, an excess level of supersaturation is needed to commence nucleation¹². The one-shot injection technique fulfils this requirement by using the precursor at a high concentration, thus enabling fast reaction kinetics at the onset.

For simplicity, we use monometallic nanocrystals as an explanatory example to discuss the kinetics of a colloidal synthesis process that typically involves the reduction of a metal precursor (M^{n+}) by a reductant to produce M^0 atoms. At the initial stage, the reaction is thought to follow a second-order rate law because the reduction requires collision and electron transfer between the precursor and reductant species involved. As such, the reduction rate is directly proportional to the concentration of both the precursor and the reductant. If the reductant is present in large excess over the precursor, the reduction can be approximated as a pseudo-first-order reaction 13 . In this case, the overall reduction rate R can be expressed as follows:

$$R = -d[M^{n+}]/dt = k \times [M^{n+}], \tag{1}$$

where $[M^{n+}]$ is the concentration of the precursor, k is the rate constant and t is time. This equation can be integrated to generate:

$$[M^{n+}] = [M^{n+}]_0 \times e^{-kt},$$
 (2)

where $[M^{n+}]_0$ is the initial concentration of the precursor. The integrated rate law is

$$R = k[\mathsf{M}^{n+}]_0 \times e^{-kt}. \tag{3}$$

According to equation (3), the reduction rate will peak at the beginning of a synthesis before any of the precursor has been reduced. As such, the rapid rise in precursor concentration associated with the one-shot injection ensures a high initial reduction rate, which, in turn, leads to the generation of a large quantity of M° atoms, triggering the formation of essentially all seeds via homogeneous nucleation within a short period of time. The simultaneous generation of all of the seeds is primarily responsible for producing nanocrystals with a narrow distribution in size. Following the emergence of the seeds, growth commences, accompanied by size enlargement and shape evolution. The final shape adopted by the nanocrystals is determined mainly by the interplay between two competing processes: atom deposition and surface diffusion. In the case of one-shot injection, the M° atoms are deposited at a relatively high rate, making the rate of surface diffusion a decisive factor in controlling the shape-evolution process.

As a typical feature associated with one-shot injection, the precursor concentration, and thus the reaction rate, is expected to undergo an exponential decay over time (Fig. 1b). Although such nonlinearity and strong dependence on the rate constant k may not notably affect the final size or shape adopted by the nanocrystals, they play a vital role in determining the spatial distributions of different elements when more than one metal is involved. The instantaneous composition of a bi- or multi-metallic nanocrystal is determined by the relative reduction rates of the corresponding precursors. When synthesizing AB alloy nanocrystals from two precursors (A^{m+} and B^{n+}) using the one-shot injection method, the composition of the resultant nanocrystal will vary constantly along the radial direction depending on the ratio between the reduction rates of the two precursors. In general, it becomes exceedingly challenging to experimentally control the composition of nanocrystals that consist of two or more metals.

In an ideal scenario, where both the precursor concentration and reaction rate constant remain the same throughout the synthesis, the M⁰ atoms will be produced at a stable rate to achieve a uniform distribution along the radial direction of a nanocrystal and thus enable precise control over the composition. However, achieving and maintaining a constant precursor concentration throughout the synthesis is practically unfeasible. One potential strategy for overcoming this limitation is to continually supply the reaction system with additional precursor to compensate for what has been consumed ¹⁴. By dividing the total precursor solution into smaller portions and introducing them into the reaction mixture as regularly paced droplets instead of injecting it all at once, it is possible to maintain the precursor concentration at a stable level.

To simplify the analysis, we adopt a model in which the precursor is added in the form of droplets of a fixed size at a specific pace while neglecting the temperature fluctuation and volume increase of the reaction mixture (Fig. 1c). In this model, the reduction of the precursor contained in individual droplets can be treated as independent events, with the concentration following the same exponential decay as observed in the case of one-shot injection. For instance, the addition of the first droplet contributes to a rapid increase in concentration, followed by the gradual decrease as described in equation (2) until the second droplet is introduced. The addition of each subsequent droplet induces a similar pattern that features a sudden increase in precursor concentration and then exponential decay (Fig. 1d). Taken together, the precursor concentration will oscillate up and down with the addition of more droplets while maintaining an overall upward trend. Mathematically, the instantaneous concentration of the precursor in the reaction mixture at time $t(c_t)$ can be expressed as the sum of contributions from all of the droplets added to this point¹⁵:

$$\begin{split} c_t &= c_0 \times e^{-kt} + c_0 \times e^{-k(t-\tau)} + c_0 \times e^{-k^{(t-2\tau)}} + \cdots \\ &+ c_0 \times e^{-k(t-N\tau)} = c_0 \times e^{-kt} (1 - e^{Nk\tau + k\tau}) / (1 - e^{k\tau}), \end{split} \tag{4}$$

Table 1 | The major differences between the one-shot injection and dropwise addition methods used to introduce the precursors

	One-shot injection	Dropwise addition
Precursor concentration	Exponential decay from a very high level to zero	Maintained at a stable, relatively low level
Variation of concentration	Continuous decay over a broad range	Oscillation within a narrow range
Tuning of concentration	k, c _o	C ₀ , τ
Preformed seeds	Typically, not involved	Typically involved
Nucleation behaviour	Homogeneous or heterogeneous	Heterogeneous only
Growth behaviour	Controlled by the deposition rate	Controlled by the diffusion rate
Size uniformity	Uniform or non-uniform	Uniform
Shape control	Kinetic shape	Kinetic or thermodynamic shape
Composition control	Continuous variation along the radial direction	Uniform across the particle and precisely tunable

where c_0 is the increase in concentration contributed by an individual droplet, τ is the interval of time between adjacent droplets and N is the total number of droplets added to the mixture up to time point t. According to equation (4), the concentration c_t is determined by the values of c_0 , k and τ . It can be readily calculated for any combination of c_0 and τ if the value of k is known.

According to equation (1), as the precursor concentration increases continually, the consumption rate of the precursor also increases proportionally. This eventually leads to a situation where the decrease in concentration caused by reduction between two adjacent droplets is adequately compensated by the increase in concentration caused by the addition of a droplet. This results in the establishment of a steady state in which the precursor concentration fluctuates between just two values defined by the upper limit ($c_{\rm up}$) and lower limit ($c_{\rm low}$), as does the reaction rate. The condition for establishing the steady state can be expressed as

$$c_0 = c_{\rm up} - c_{\rm up} \times e^{-k\tau} = c_{\rm up}(1 - e^{-k\tau}).$$
 (5)

From equation (5), we can derive c_{up} as

$$c_{\rm up} = c_0/(1 - e^{-k\tau}),$$
 (6)

and c_{low} as

$$c_{\text{low}} = c_{\text{up}} \times e^{-k\tau} = c_0 \times e^{-k\tau}/(1 - e^{-k\tau}).$$
 (7)

The average concentration (c_{avg}) in the steady state can be calculated as the total area under the decay curve between two adjacent droplets divided by τ :

$$\begin{aligned} c_{\text{avg}} &= \int_0^\tau c_{\text{up}} \times e^{-kt} \times \text{d}t/\tau = \int_0^\tau \left[c_0/(1-e^{-k\tau}) \right] \times e^{-kt} \times \text{d}t/\tau \\ &= c_0/(k \times \tau). \end{aligned} \tag{8}$$

To illustrate the differences between one-shot and dropwise injection modes, let us examine an imaginary synthetic scenario involving a set of experimental parameters. In the case of one-shot injection (Fig. 1b), the added precursor contributes to a total concentration of 1 M in the reaction mixture. For dropwise addition (Fig. 1d), the precursor

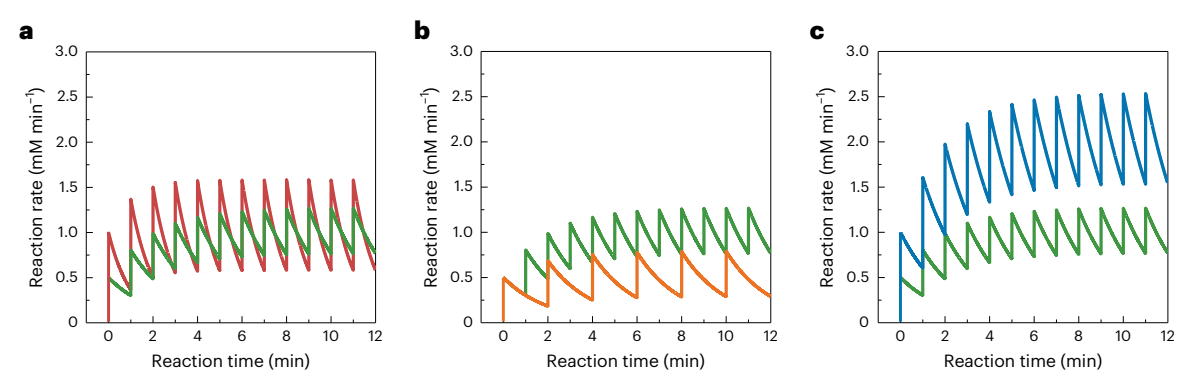


Fig. 2 | Plots illustrating the respective influence of k, τ and c_0 on the instantaneous concentration of a precursor. a-c, Compared with the green curve (which is the same as that in Fig. 1d), the value of k is increased to 1.0 min⁻¹(a), the value of τ is increased to 2 min (b) and the value of c_0 (the increase in precursor concentration when one droplet is added) is increased to 2 mM (c).

solution is divided into 1,000 droplets and added at a controlled pace so that τ is 1 min. The rate constant k is set to 0.5 min⁻¹ in both cases. These parameters enable us to compare the temporal profiles of the precursor concentration and reaction rate under the two types of injection mode.

For one-shot injection, the precursor concentration rapidly reaches a level of 1 M. Concurrently, the reduction reaction leads to a rapid decay in the precursor concentration. According to equation (2), as shown in terms of c and c_0 in the equation alongside the temporal profile in Fig. 1b, the half-life ($t_{1/2}$) of this pseudo-first-order reaction can be calculated as

$$t_{1/2} = (\ln 2)/k = 1.4 \text{ min},$$
 (9)

indicating that half of the added precursor will have been consumed after only 1.4 min from the start of the synthesis. Notably, the reaction will be nearly completed at t=10 min as the precursor concentration approaches zero.

By contrast, when the precursor is supplied as a train of droplets through dropwise addition, its concentration can be maintained at a much lower but relatively stable level throughout the synthesis. Upon addition of the first droplet, the concentration reaches a modest peak of 1.0 mM, which is equivalent to 1‰ of the concentration associated with one-shot injection. When the eighth droplet is added, a steady state will be established, reaching the maximum concentration (that is, the upper limit, $c_{\rm up}$) of 2.5 mM. It is worth noting that the upper limit is 400 times lower than the maximum concentration involved in one-shot injection. The average concentration in the steady state can therefore be calculated as 2.0 mM using equation (8). The temporal profile in Fig. 1d covers only the initial 12 min of the synthesis. In reality, dropwise addition can stretch over several hours, with almost the entire synthesis dominated by the steady-state reaction conditions.

Dropwise addition of precursor(s) offers many immediate advantages over one-shot injection. First of all, the use of precursor(s) at a low concentration ensures a low level of supersaturation and thus enables the elimination of homogeneous nucleation when preformed seeds are present, leading to products with a uniform size distribution 16. In addition, the generation of M⁰ atoms at a constant and controlled rate enables the derivation of the growth rate by developing geometric models that incorporate parameters such as the dimensions and lattice constants of the seed, as well as the deposition rate (given as the number of M⁰ atoms per seed). In terms of shape control, a quantitative knowledge of the reaction rate offers a direct means for kinetic control of the shape evolution during growth, as discussed in several review articles¹⁷. As for control of the composition, the dropwise addition of several precursors offers a reliable method for regulating their relative reaction rates. A discussion of experimental control over the composition is presented in the next section. Table 1 shows a summary of the major differences between one-shot injection and dropwise addition for the colloidal synthesis of nanocrystals.

Controlling the composition of bimetallic nanocrystals

For the synthesis of bi- and multi-metallic nanocrystals, achieving a steady state is only the first step in the quest for compositional control. The final composition of the nanocrystals is governed by the reduction rates of the precursors involved, with the reduction rate being a product of the precursor concentration and the reaction rate constant:

$$R = k \times c_t. \tag{10}$$

From equations (6)–(8) and (10), the upper limit ($R_{\rm up}$), lower limit ($R_{\rm low}$) and average value ($R_{\rm avg}$) of the reduction rate in the steady state can be derived as:

$$R_{\rm up} = k \times c_0/(1 - e^{-k\tau}),$$
 (11)

$$R_{\text{low}} = k \times c_0 \times e^{-k\tau} / (1 - e^{-k\tau}),$$
 (12)

$$R_{\rm avg} = c_0/\tau. (13)$$

Although R_{up} and R_{low} are still defined by the same three parameters of c_0 , k and τ , R_{avg} is solely dependent on c_0 and τ , not on k. Therefore, the reactivity of a precursor becomes inconsequential in determining its reaction rate. This unique feature of dropwise addition holds immense value in experimentally controlling the composition of a nanocrystal, as it enables precise tuning of the elemental ratio by simply adjusting the concentrations and/or injection rates of the precursors, regardless of their intrinsic reactivity. This simplicity and versatility in terms of experimental control is advantageous. For example, when k is increased from 0.5 to 1.0 min⁻¹ (Fig. 2a), the range of variation in the reaction rate expands from 0.75-1.25 mM min⁻¹ to 0.60-1.60 mM min⁻¹ due to the changes in $R_{\rm up}$ and $R_{\rm low}$. However, $R_{\rm avg}$ remains at 1.0 mM min⁻¹, implying that the overall deposition rate of M⁰ atoms remains unaffected despite the increased reactivity of the precursor. As such, when the precursor solutions of two different metals are prepared with the same concentration and added to the growth solution dropwise at the same injection rate, alloy nanocrystals with an elemental ratio of 1:1 will always be obtained.

In comparison with k, both τ and c_0 have a greater influence on the reduction rate in the steady state. Increasing τ from 1 to 2 min reduces the frequency of the oscillating curve (Fig. 2b). Meanwhile, it induces an inversely proportional decrease in $R_{\rm avg}$ and increases the range of variation through complicated mechanisms, as indicated by equations (11) and (12). Overall, it is pivotal to keep τ as short as possible,

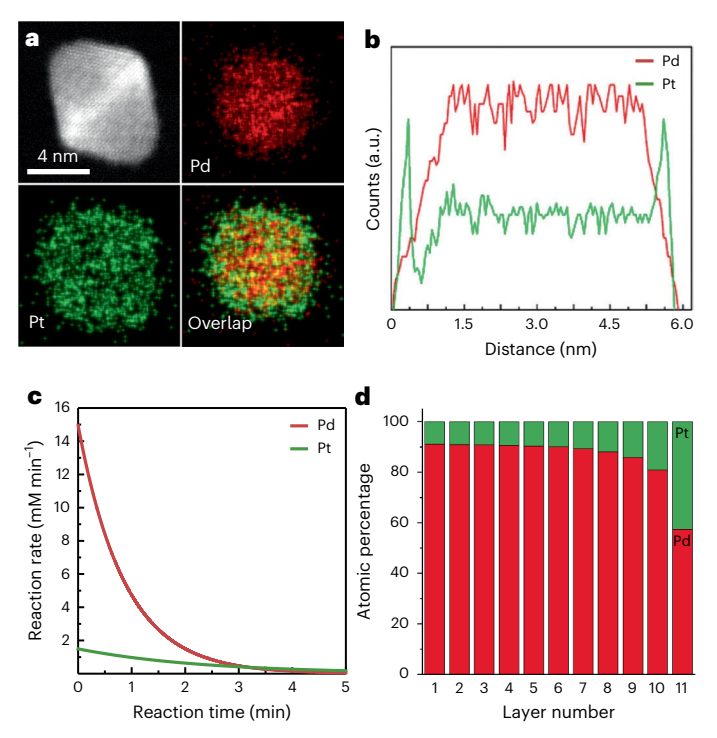
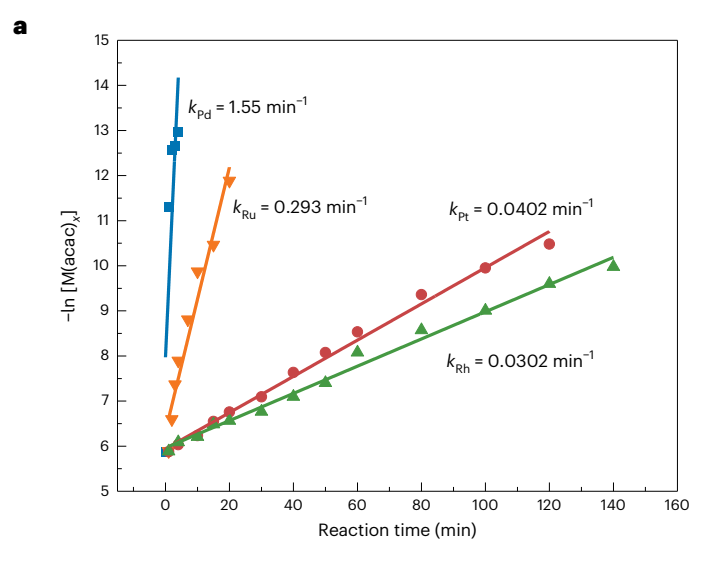


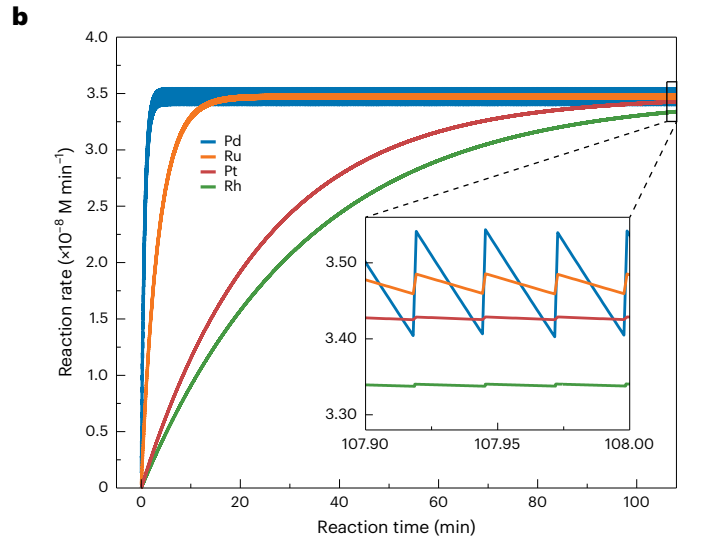
Fig. 3 | **Non-uniform elemental distribution in the products obtained using one-shot injection. a,b**, Scanning transmission electron microscopy image, elemental mapping images (**a**) and EDX analyses (**b**) of a Pd@Pt core-shell nanocrystal obtained through one-shot injection. **c**, Reaction rates of the Pd(II) and Pt(II) precursors as a function of the reaction time. **d**, Simulated composition in each atomic layer of a core-shell octahedron. Panels **a** and **b** adapted with permission from ref. 18, American Chemical Society.

especially when highly reactive precursors are used for the synthesis. This requirement can be met experimentally by increasing the injection rate, applying a nozzle with a smaller diameter, using a solvent with a lower viscosity to generate finer droplets or a combination of these methods. Nevertheless, the last two approaches may encounter technical challenges and material limitations during operation. If the reaction rate is controlled by adjusting τ , separate precursor solutions and several injection systems will be necessary.

As illustrated in Fig. 2c, increasing c_0 from 1 to 2 mM results in a proportional increase in $R_{\rm up}$, $R_{\rm low}$ and $R_{\rm avg}$, offering a straightforward handle for controlling the reaction rate without compromising its stability. Notably, the technical simplicity offers an additional advantage, as c_0 of each precursor can be easily controlled over a broad range by adjusting the concentration of the precursor in the stock solution, with its solubility being the upper limit. Different precursors can also be prepared as a single mixture and injected using the same fluidic system set-up. By controlling the molar ratio between different precursors, the composition of the resultant bi- or multi-metallic nanocrystals can be finely tuned.

The role played by the mode of precursor injection in controlling the composition of metal nanocrystals can be understood through analysis using energy-dispersive X-ray (EDX) spectroscopy and mathematical simulations. The sample in this study was prepared through one-shot injection, where a mixture of Pd(II) and Pt(II) precursors was quickly introduced. The resulting nanocrystals exhibited a core–shell structure, with Pd concentrated in the core and Pt deposited as a conformal shell 18. This elemental distribution can be attributed to the much greater reactivity of the Pd(II) precursor ($k_{\rm Pd} = 1.15 \, {\rm min}^{-1}$) relative to that of the Pt(II) precursor ($k_{\rm Pt} = 0.427 \, {\rm min}^{-1}$). The one-shot injection promoted the generation of abundant Pd atoms, leading to the formation of a Pd-rich core (Fig. 3a,b). To account for the non-uniform elemental





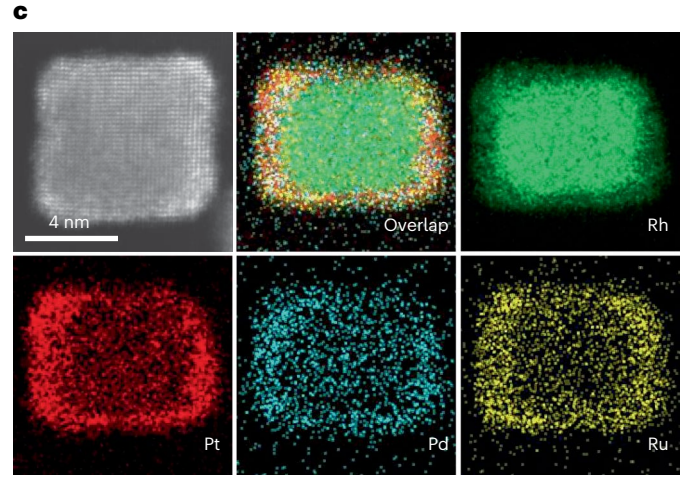


Fig. 4 | **Controlling the composition of high-entropy alloy nanocrystals through dropwise addition. a**, Plots showing the linear relationship between $-\ln[M(acac)_x]$ (M = Pd, Ru, Pt, Rh) and the reaction time and the fittings based on the pseudo-first-order kinetics measured using inductively coupled plasma mass spectrometry. b, Simulated precursor reaction rate as a function of the reaction time in the case of dropwise addition. **c**, Scanning transmission electron microscopy image and EDX elemental mapping of an alloy nanocrystal, showing the spatial distributions of Rh, Pt, Pd and Ru. Panels **a**–**c** adapted with permission from ref. 14, American Chemical Society.

distribution, we plotted the reaction rates (derived from the concentration and rate constant of the precursor) as a function of the reaction time. The plot in Fig. 3c clearly indicates that the reduction of the Pd(II) precursor proceeded at a much faster rate, whereas the production of Pt atoms was stretched over a much longer period of time. Figure 3d shows the simulated layer-by-layer compositional profiles. Consistent with the experimental data, the profiles show a Pd-dominant core and a gradual increase in Pt content towards the outer surface.

Extension to high-entropy alloy nanocrystals

High-entropy alloys, which contain five or more elements, have attracted ever-increasing attention due to their inherent complexity in composition and thus the multitude of possible atomic configurations¹⁹. These alloys offer a productive platform for the development of advanced heterogeneous catalysts^{20,21}. However, controlling the composition of high-entropy alloys is more challenging compared with the bimetallic system. For high-entropy alloys, not only are the precursors characterized by diverse reactivities but also the constituent metals themselves possess distinct physicochemical properties, such as bond energies, stacking-fault energies and chemical stabilities, and may even crystallize in different phases^{22,23}. Controlling the elemental compositions of high-entropy alloy nanocrystals requires a synthetic approach that can be universally applied to a large number of different metals. The dropwise addition method holds promise for enabling the precise and controllable fabrication of a variety of high-entropy alloy nanocrystals. The decoupling between the precursor reactivity and the steady-state reaction rate may save time when optimizing the experimental variables required for tuning the reactivity of each precursor.

In a preliminary exploration, the dropwise addition method has been successfully applied to enable the synthesis of nanocrystals made of a quaternary alloy (Fig. 4)¹⁴. To avoid any detrimental effect from oxidative etching, four acetylacetonate (acac) complexes were chosen as halide-free precursors of Ru, Rh, Pd and Pt, despite their large difference in reactivity (Fig. 4a). The use of Rh nanocubes as templates aided in shaping the alloy nanocrystals and thus controlling the surface facet. To reconcile the varying reduction kinetics of these precursors, a carefully designed system for precursor introduction was implemented. This system enabled the precursor mixture to be introduced into the reaction system in the form of tiny droplets that contained only about 2.2 nmol of each metal per droplet. In this way, the reduction rates of the different precursors were made equal after 1 h into the synthesis (Fig. 4b), facilitating the synthesis of Ru–Rh–Pd–Pt alloy nanocrystals with a uniform composition towards the surface (Fig. 4c).

For dropwise synthesis, the reaction should be quenched immediately following the addition of the last droplet by rapidly cooling the reaction mixture to room temperature. If the reaction is allowed to continue, the remaining precursors will revert to individual exponential decays similar to the case of one-shot injection, affecting the surface composition. Nevertheless, such an impact may be negligible given that the precursors are at much lower concentrations than in one-shot synthesis.

Outlook

Dropwise addition provides a robust route to the colloidal synthesis of bi- and multi-metallic nanocrystals with uniform, controllable and even predictable compositions that are determined by the reduction rates of the corresponding precursors in the steady state. When conformally deposited on preformed seeds of various shapes as overlayers with a thickness of a few atomic layers, nanocrystals with well-defined surface structures (in both composition and atomic arrangement) will be obtained. Such nanocrystals not only offer a class of well-controlled materials to investigate the structure–property relationships but also provide a great opportunity to develop next-generation catalysts with enhanced activity, selectivity and/or durability.

It is worth emphasizing that our discussion about composition control is primarily from the synthetic perspective. The difficulty associated with the atomic characterization of an alloy nanocrystal's composition makes it extremely challenging to elucidate the structure–property relationships, particularly with regard to the elemental distribution in these nanoscale materials. This Perspective underscores the need for increased research investment from synthetic chemists to gain mechanistic insights and experimental control over the chemical processes that determine the compositions and elemental distributions of nanocrystals. In addition, it calls for efforts to develop advanced techniques for compositional analysis, which hold the key to both rational and deterministic synthesis.

References

- Pearce, A. K., Wilks, T. R., Arno, M. C. & O'Reilly, R. K. Synthesis and applications of anisotropic nanoparticles with precisely defined dimensions. *Nat. Rev. Chem.* 5, 21–45 (2021).
- Chen, R., Lyu, Z., Shi, Y. & Xia, Y. Improving the purity and uniformity of Pd and Pt nanocrystals by decoupling growth from nucleation in a flow reactor. *Chem. Mater.* 33, 3791–3801 (2021).
- 3. Zheng, Y., Zhong, X., Li, Z. & Xia, Y. Successive, seed-mediated growth for the synthesis of single-crystal gold nanospheres with uniform diameters controlled in the range of 5–150 nm. *Part. Part. Syst. Charact.* **26**, 13890–13895 (2020).
- Shi, Y. et al. Noble-metal nanocrystals with controlled shapes for catalytic and electrocatalytic applications. Chem. Rev. 121, 649–735 (2021).
- Bin, D. S. et al. Controlling the compositional chemistry in single nanoparticles for functional hollow carbon nanospheres. *J. Am. Chem. Soc.* 139, 13492–13498 (2017).
- Link, S., Wang, Z. & El-Sayed, M. A. Alloy formation of gold-silver nanoparticles and the dependence of the plasmon absorption on their composition. J. Phys. Chem. B 103, 3529–3533 (1999).
- Stamenkovic, V. R. et al. Improved oxygen reduction activity on Pt₃Ni(111) via increased surface site availability. Science 315, 493–497 (2007).
- Yao, Y. et al. Carbothermal shock synthesis of high-entropy-alloy nanoparticles. Science 359, 1389–1394 (2018).
- 9. Tong, K. et al. Structural transition and migration of incoherent twin boundary in diamond. *Nature* **626**. 79–85 (2024).
- Swallow, J. E. N. et al. Revealing the role of CO during CO₂ hydrogenation on Cu surfaces with in situ soft X-ray spectroscopy. J. Am. Chem. Soc. 145, 6730–6740 (2023).
- 11. Fan, L. et al. High entropy alloy electrocatalytic electrode toward alkaline glycerol valorization coupling with acidic hydrogen production. *J. Am. Chem. Soc.* **144**, 7224–7235 (2022).
- Lamer, V. K. & Dinegar, R. H. Theory, production and mechanism of formation of monodispersed hydrosols. *J. Am. Chem. Soc.* 72, 4847–4854 (1950).
- Corbett, J. F. Pseudo first-order kinetics. J. Chem. Educ. 49, 663 (1972).
- Wang, C. et al. Facet-controlled synthesis of platinum-groupmetal quaternary alloys: the case of nanocubes and {100} facets.
 J. Am. Chem. Soc. 145, 2553–2560 (2023).
- Peng, H. C., Park, J., Zhang, L. & Xia, Y. Toward a quantitative understanding of symmetry reduction involved in the seed-mediated growth of Pd nanocrystals. J. Am. Chem. Soc. 137, 6643–6652 (2015).
- 16. Zhang, D. et al. Dropwise addition of cation solution: an approach for growing high-quality upconversion nanoparticles. *J. Colloid. Interface Sci.* **512**, 141–150 (2018).
- Nguyen, Q. N., Wang, C., Shang, Y., Janssen, A. & Xia, Y. Colloidal synthesis of metal nanocrystals: from asymmetrical growth to symmetry breaking. *Chem. Rev.* 123, 3693–3760 (2023).

- Zhou, M. et al. Quantitative analysis of the reduction kinetics responsible for the one-pot synthesis of Pd–Pt bimetallic nanocrystals with different structures. J. Am. Chem. Soc. 138, 12263–12270 (2016).
- George, E. P., Raabe, D. & Ritchie, R. O. High-entropy alloys. Nat. Rev. Mater. 4, 515–534 (2019).
- Li, K. & Chen, W. Recent progress in high-entropy alloys for catalysts: synthesis, applications, and prospects. *Mater. Today Energy* 20, 100639 (2021).
- 21. Xin, Y. et al. High-entropy alloys as a platform for catalysis: progress, challenges, and opportunities. ACS Catal. **10**, 11280–11306 (2020).
- Zhao, M. & Xia, Y. Crystal-phase and surface-structure engineering of ruthenium nanocrystals. *Nat. Rev. Mater.* 5, 440–459 (2020).
- 23. Chen, P. C. et al. Polyelemental nanoparticle libraries. *Science* **352**, 1565–1569 (2016).

Acknowledgements

This work was supported in part by a research grant (DMR 2333595) from the NSF and start-up funds from the Georgia Institute of Technology. We are grateful to our co-workers and collaborators for their invaluable contributions to this project.

Author contributions

This Perspective was conceived by Y.X. and was written by C.W., J.H. and Y.X.

Competing interests

The authors declare no competing interests.

Additional information

Correspondence should be addressed to Younan Xia.

Peer review information *Nature Synthesis* thanks Xuelian Chen and Svetlana Neretina for their contribution to the peer review of this work. Primary Handling Editor: Alexandra Groves, in collaboration with the *Nature Synthesis* team.

Reprints and permissions information is available at www.nature.com/reprints.

Publisher's note Springer Nature remains neutral with regard to jurisdictional claims in published maps and institutional affiliations.

Springer Nature or its licensor (e.g. a society or other partner) holds exclusive rights to this article under a publishing agreement with the author(s) or other rightsholder(s); author self-archiving of the accepted manuscript version of this article is solely governed by the terms of such publishing agreement and applicable law.

© Springer Nature Limited 2024